Electrostatic Potential Screened by a Two-Dimensional Electron System: A Real-Space Observation by Scanning-Tunneling Spectroscopy

Masanori Ono,[1] Y. Nishigata,[1] T. Nishio,[1] T. Eguchi,[1] and Y. Hasegawa[1,2,*]

[1]*The Institute for Solid State Physics, The University of Tokyo, 5-1-5 Kashiwa-no-ha, Kashiwa, 277-8581, Japan*

[2]*PRESTO, Japan Science and Technology Agency, Japan*

(Received 23 June 2005; published 6 January 2006)

Scanning-tunneling spectroscopy at 5 K was used to investigate the electrostatic potential profile on the Si(111)-$\sqrt{3} \times \sqrt{3}$ Ag surface at subnanometer spatial resolution. The potential was measured from an energy-level shift of electronic states on the surface. The potential images obtained reveal that the potential drops around the steps and Ag adsorbates, upon which positive charges are presumably accumulated. The profiles of the reduced potentials are explained with the screening of potential due to the charges by two-dimensional electron gas (2DEG) existing on the surface. The Friedel oscillation, which results from the screening and has a period of the half Fermi wavelength of the 2DEG, was also observed in the potential images.

DOI: 10.1103/PhysRevLett.96.016801 PACS numbers: 73.20.Hb, 68.37.Ef, 73.25.+i, 73.90.+f

When a positive charge is placed in an electron gas, the electrons in the gas gather around the charge, trying to compensate for the electrostatic potential it has induced. This phenomenon, called screening, is one of the simplest and most important manifestations of electron-electron interaction [1]. Modifying various interactions and scattering potentials, screening plays a crucial role in the emergence of various material properties. In this Letter, we report on the direct real-space visualization of the screening phenomena by two-dimensional electron gas (2DEG) on a surface [2,3], which was achieved using scanning-tunneling microscopy or spectroscopy (STM or STS) through observation of the electrostatic potential on the surface at subnanometer spatial resolution. The characteristic features of the screening, such as the decaying potential and Friedel oscillation [4], are clearly observed in the potential images. As far as we know, this is the first real-space observation of screening phenomena on a microscopic scale.

As a sample having 2DEG we used the Si(111)-$\sqrt{3} \times \sqrt{3}$ Ag ($\sqrt{3}$ Ag for short) surface, whose typical STM image is shown in Fig. 1(a). The surface has been extensively studied [5] because of its unique structural and electronic properties, such as a controversial structural phase transition around 150 K [6]. It has a few surface states below the Fermi energy E_F; S_1 and S_2/S_3 (degenerated at the $\bar{\Gamma}$ point), revealed by angle-resolved photoemission spectroscopy (ARPES) [7–9]. The S_1 state is metallic with isotropic paraboloidal energy dispersion, producing a free-electron-like electron system or 2DEG on the surface. Electron standing wave patterns [10,11], characteristic to the surface 2DEG, are observed in tunneling conductance (dI/dV) images, as shown in Fig. 1(b) [12], which represent a mapping of the local density of states (LDOS) of the surface.

Actually, the binding energy of the S_1 state ranges from 0 to -0.3 eV with respect to E_F, depending on the ARPES measurements, while the energy difference between the S_1 and S_2/S_3 states is rigidly maintained (~ 0.7 eV) [7–9]. It is currently believed that the variation is due to a potential shift, induced by a charge donation from excess Ag atoms on the surface into the surface states [8,9,13]. The reason why the shift varies with the measurements is that the amount of the excess Ag atoms depends on the sample preparation conditions, such as the postannealing temperature. In fact, intentional Ag deposition on the $\sqrt{3}$ Ag surface shifts the binding energy of the surface states to a

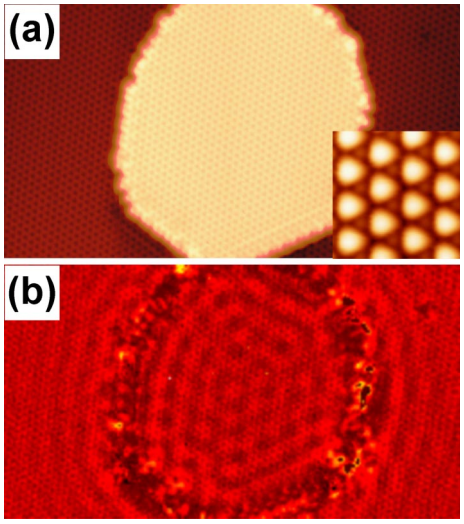

FIG. 1 (color online). (a) Empty-state STM and (b) dI/dV images of the Si(111)-$\sqrt{3} \times \sqrt{3}$ Ag surface taken at 5 K on the same area. The imaged dI/dV values were numerically calculated at a sample bias voltage V_s of $+0.3$ V from the I-V spectra taken with the 2DTS method. The size of the images is 23 nm $\times$ 40 nm. V_s and tunneling current I_t are -1.5 V and 200 pA, respectively, for the STM imaging (a) and for the feedback stabilization (b). The inset in (a) is a zoomed filled-state STM image of size 2.25 nm $\times$ 2.25 nm (V_s: -0.1 V; I_t: 300 pA), clearly showing the IET structure.

higher energy site [8]. These facts indicate that, by measuring the energy level of the surface states, we can measure the potential on the surface and, by performing the measurement in a two-dimensional manner, using STS, we can obtain its spatial mapping at subnanometer spatial resolution. Here, we measured the potential mapping in the area where the excess Ag atoms are located, such as around Ag clusters and surface step edges since local variation of the potential is expected there.

For the measurements we used ultrahigh vacuum (UHV) low temperature STM (USM-1300, Unisoku, and SPM-1000, RHK), in which the tip and sample can be cooled with liquid He. All the STM images and spectroscopic data shown in this Letter are taken at 5 K in UHV. The details of the instrumentation were reported in our previous paper [14]. A clean Si(111)-7 × 7 surface was prepared by annealing a piece of highly doped silicon wafer (As doped, n-type, $1 \sim 6 \times 10^{17}$ cm^{-3}) above 1200 °C. The $\sqrt{3}$ Ag structure was then formed by the deposition of ≥ 1 monolayer of Ag on the clean surface and successive annealing at 600 °C for ~5 min. STM images taken after the annealing exhibit a $\sqrt{3} \times \sqrt{3}$ structure described with an inequivalent triangular (IET) model [6], as shown in the STM images of Fig. 1(a) and its inset. On this surface, we performed two-dimensional tunneling spectroscopy (2DTS) measurement, that is, a measurement of a tunneling-current spectrum (I-V curve) with the STM feedback loop turned off at each point during scanning of the tip over the surface. From these spectra we can easily make the dI/dV LDOS images, such as that shown in Fig. 1(b), and a mapping of the peak energy of the specific electronic state in the dI/dV spectrum, which corresponds to the electrostatic potential image.

A measured potential profile around a step edge of the $\sqrt{3}$ Ag structure is shown in Fig. 2. Figure 2(a) is an STM image around the lower side of the step edge. The inset shows a series of normalized dI/dV spectra taken at the positions indicated by the arrows in the STM image. The peak around −0.85 V, which is attributed to the S_2/S_3 states, shifts to the higher binding energy (lower sample bias voltage) side as the measured site approaches the step edge [15]. The shift is due to the potential change, as mentioned above. A mapping of the peak energy shift of the S_2/S_3 states extracted from the 2DTS data is shown in Fig. 2(b), representing a potential distribution in the area where the $\sqrt{3}$ Ag structure is formed. It obviously exhibits lowered potential near the step edge. A cross-sectional plot of the potential, which was obtained by averaging the potential profiles along the step edge, is presented in Fig. 2(c), together with a topographic profile. The solid line is the potential profile, calculated from a theory of the screening, showing excellent correlation with the measured one.

Before going into details of the screening theory and the fitting procedure, it should be noted here that this potential measurement method is effective only on the area where

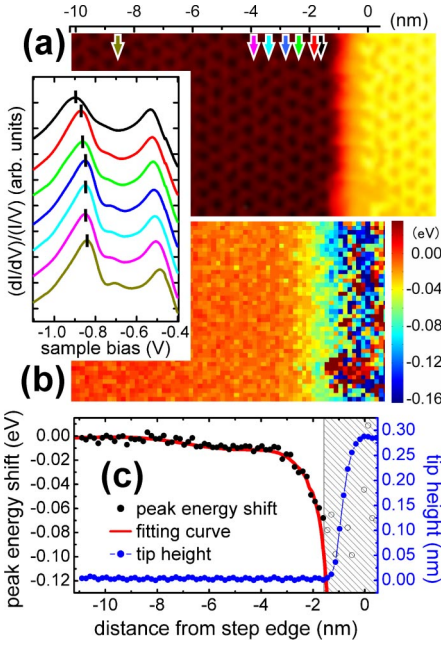

FIG. 2 (color online). (a) An STM image and (b) a mapping of the peak energy shift of the S_2/S_3 states near a lower step edge on the $\sqrt{3}$ Ag surface. The inset plots normalized dI/dV spectra, measured at the sites marked in the STM image. Conditions for the STM and 2DTS measurements are the same as Fig. 1. (c) Cross-sectional plots of the topograph and the peak energy shift as a function of distance from the step edges. To make the dI/dV spectra in the inset and the two profiles in (c), 42 sets of data are averaged along the step edge.

the $\sqrt{3}$ Ag structure is formed, since the measurement employs an energy level of surface states attributed to the structure. For instance, at the step [the hatched area in Fig. 2(c)], the $\sqrt{3}$ Ag structure is not formed, and thus data points in the area do not represent the potential. For the same reason, tiny fluctuations, reflecting a unit cell of the $\sqrt{3}$ Ag structure and found vaguely in the measured potential image [Fig. 2(b)], are not real either.

According to the theory of screening [1], the response of an electronic system to an external charge is described in terms of its dielectric function. The static dielectric function of 2DEG as a function of wave number q is calculated from the Lindhard function as follows [2,3]:

$$\epsilon_{\mathrm{r}}(q) = \begin{cases} 1 + \frac{2}{qa_B} & (q \leq 2k_{\mathrm{F}}) \\ 1 + \frac{2}{qa_B}\{1 - [1 - (\frac{2k_{\mathrm{F}}}{q})^2]^{1/2}\} & (q > 2k_{\mathrm{F}}) \end{cases}, \quad (1)$$

where a_B ($= 4\pi\epsilon\hbar^2/m^*e^2$) is the effective Bohr radius and k_{F} is the wave number of the 2DEG at E_{F}. Here m^* is the effective mass of electrons in 2DEG. The dielectric constant of the surrounding materials, ϵ, is the average of dielectric constants of the vacuum and silicon substrate in our case [2,3,16]. As will be discussed later, we found the value of k_{F} 0.45 nm^{-1} on the surface.

The potential due to the point charge screened by the 2DEG is calculated by two-dimensional inverse Fourier

transformation of $V_{2D}(q)/\epsilon_r(q)$ [2], where $V_{2D}(q)$ $(= e^2/2\epsilon q)$ is the two-dimensional Fourier transform of the Coulomb potential. In order to obtain the potential around step edges, the numerically calculated screened potential of the point charge was integrated by assuming linearly arranged charges along the step edges of the measured area. The resulting potential was fitted with the measured one as shown in Fig. 2(c). The parameters adjusted for fitting are the linear charge density at the step edges (0.55 electrons/nm), which is, in fact, included in the proportional coefficient of the potential profile, the origin of the peak energy shift (-0.85 V), and the position of the linear charges (-1.3 nm from the upper step edges). The fitting result clearly demonstrates that the measured potential profile is indeed due to the screening.

In order to confirm that the observed potential variation is due to the screening, we also measured the potential around an Ag cluster, using the same method as we did for the step edges. A silver cluster called ''propeller'' [17] is found in the empty-state (a) and filled-state (b) STM images shown in Fig. 3. The potential images taken around the cluster [Figs. 3(c) and 3(e)] and its cross-sectional plots along the lines drawn in the larger potential image [Figs. 3(f) and 3(g)] are also presented in Fig. 3. Since the atomic structure and the number of Ag atoms in the cluster remain unsolved, we assumed that three Ag atoms were situated at the peak sites in the potential images [17]. These sites are the center of the three small Ag triangles in the IET model, as schematically shown in Fig. 3(d).

Subsequently, we carried out a fitting with the sum of three screened potential functions, whose origin is set at the Ag atom site. Since the surface was newly prepared and thus different from that shown in Fig. 2, we measured the Fermi wave number k_F again from an LDOS image at E_F taken on the present surface and found 0.95 nm^{-1}. As the case of Fig. 2, the fitting parameters are a scaling factor proportional to the charge density of the Ag atoms and the origin of the peak energy shift (-0.85 V). The fitting results plotted in Figs. 3(f) and 3(g) show positive correlation with our measurements; proving that our interpretation is correct [18]. Slight deviations due to neighboring clusters are found around the edges of the potential image and the plots. The amount of charges calculated from the scaling factor is $0.65e$ per atom [19]. It should be mentioned that the estimated amount is the total charge felt by the 2DEG. Since the total charge is closely related to the charge distribution, it cannot be simply compared with the amount of charge transfer from adsorbates, which was estimated to be 1 electron per atom for the cluster in a photoemission study [8].

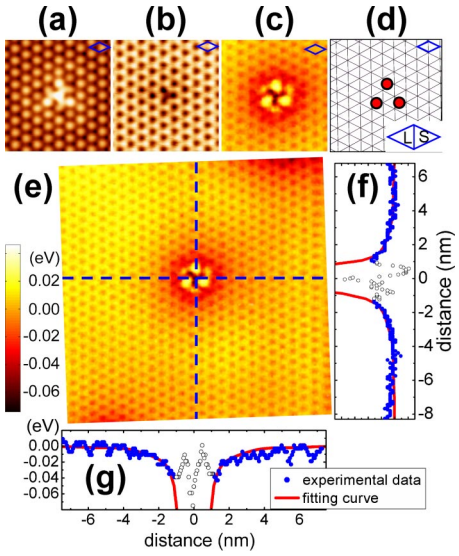

FIG. 3 (color online). (a) Empty-state STM (V_s: 1.2 V; I_t: 300 pA), (b) filled-state STM (V_s: -1.5 V, I_t: 200 pA), and (c) the potential images around an Ag cluster with its schematic (d). The unit cell of the $\sqrt{3}$ structure, of side length 0.67 nm, is marked at an identical site of each image. L and S in the schematic mean large and small Ag triangles, respectively, in the IET structural model [6]. The schematic indicates the positions at which the potential image peaks and in which we assumed the extra Ag atoms to be located. (e) A large-size (15 nm $\times$ 15 nm) potential image including the Ag cluster. The potential images, (c) and (e), were produced by 2DTS under the same conditions as Fig. 1(b). (f),(g) Potential profiles measured along the lines drawn in the large potential image. Simulated profiles are also shown.

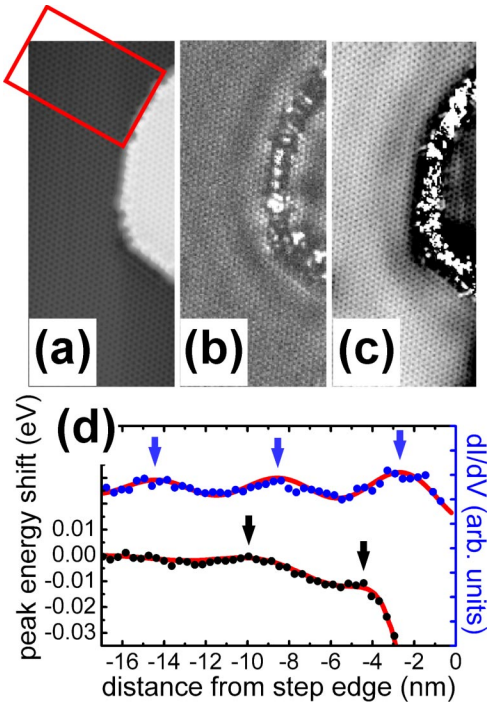

FIG. 4 (color online). (a) STM, (b) LDOS (dI/dV at $V_s = 0$), and (c) potential images taken on the same area (35 nm $\times$ 15 nm) of the $\sqrt{3}$ Ag surface. Conditions for the STM and the 2DTS measurements are the same as Fig. 1. (d) Cross-sectional plots of the LDOS and the potential, which were calculated by averaging the profiles in a box depicted in the STM image (a). Fitting curves for both profiles are drawn. The peak positions of the profiles are indicated with arrows.

The 2DEG dielectric function [Eq. (1)] indicates a cutoff of the screening effect for $q > 2k_F$ [3]. The cutoff leads to damped oscillation in the electrostatic potential with a period of half Fermi wavelength, that is, the Friedel oscillation. Indeed, in the potential images taken within an area wider than Fig. 2, we found oscillatory features that resemble the standing wave patterns observed in LDOS images. In Fig. 4, three images, (a) an STM image, (b) an LDOS image at E_F (dI/dV at $V_s = 0$), and (c) a potential image taken on the same area, are presented. In the LDOS image [Fig. 4(b)], the standing wave pattern is clearly visible. From a fitting of its cross-sectional plot with a function of the standing waves, $1 - J_0(2k_F r + \phi)$ [Fig. 4(d)], where J_0 is the zero-order Bessel function, the Fermi wavelength of the 2DEG measures $\sim$14 nm ($k_F = 0.45\ \mathrm{nm}^{-1}$). The numerically calculated potential, using the Fermi wavelength and the fitting parameters as in Fig. 2, correlates nicely with the measured potential profile shown in Fig. 4(d). This is clear evidence of the Friedel oscillation.

It should be emphasized here that the observed Friedel oscillation is different from the standing waves [10,11]. The standing waves are misleadingly referred to as energy-resolved Friedel oscillation or, simply and imprecisely, as the Friedel oscillation. They are the modulated LDOS, formed by scattering and interference in 2DEG while the genuine Friedel oscillation [4] is a spatial modulation in a total charge density or electrostatic potential caused by the screening. In this Letter, both the oscillatory patterns are presented, but only what we call the Friedel oscillation is genuine. To date, various reports have been published on the observation of the Friedel oscillation in STM. All of them are, however, actually observations of standing waves when correctly defined. We thus believe that our study is the first real-space visualization of the Friedel oscillation.

As indicated with arrows in Fig. 4(d), the peak positions of the potential oscillation are slightly shifted compared to those of the standing wave. The phase difference, 10%–15% of the period, arises from their different origins. The phase of the standing wave depends on the scattering potential while that of the potential oscillation is related to charges. The different phase and characteristic decay of the potential indicates that potential profiles are not necessarily the same as LDOS. In fact, after the observation of the standing waves [10,11], various related phenomena, such as the surface-state-mediated adatom-adatom or adatom-step interactions [20–23], were discussed in relation to the LDOS modulation since their characteristic distances seem to be related to the Fermi wavelength. Obviously the modulated electrostatic potential affects the interactions and thus should be included in their analyses. Investigation of the surface potential and its real-space imaging are therefore quite important to understand these nanoscale and atomistic phenomena on the surfaces.

In this Letter, we have demonstrated that the surface potential of the $\sqrt{3}$ Ag surface can be measured from the peak energy of surface states. From the potential mapping, we found that the potential was lowered around sites where Ag atoms had accumulated. The reduced potential is explained with the screening by the 2DEG on the surface. The Friedel oscillation was, for the first time, observed in the potential mapping.

The authors acknowledge Satoshi Watanabe, Shuji Hasegawa, Tadaaki Nagao, and Akira Endo for their fruitful discussion. This work was partly supported by a Grant-in-Aid for Scientific Research (No. 13NP0201 and No. 17360018) from the Ministry of Education, Science, Sports, and Culture of Japan, Toray Science Foundation, and Futaba Electronics Memorial Foundation.

*Electronic address: hasegawa@issp.u-tokyo.ac.jp

[1] N. W. Ashcroft and N. D. Mermin, *Solid State Physics* (Saunders College, Philadelphia, 1976).
[2] J. H. Davies, *The Physics of Low-Dimensional Semiconductors* (Cambridge University Press, Cambridge, 1998).
[3] T. Ando *et al.*, Rev. Mod. Phys. **54**, 437 (1982).
[4] J. Friedel, Nuovo Cimento Suppl. **7**, 287 (1958).
[5] S. Hasegawa, J. Phys. Condens. Matter **12**, R463 (2000).
[6] H. Aizawa *et al.*, Surf. Sci. **429**, L509 (1999).
[7] L. S. O. Johansson *et al.*, Phys. Rev. Lett. **63**, 2092 (1989).
[8] Y. Nakajima *et al.*, Phys. Rev. B **56**, 6782 (1997).
[9] X. Tong *et al.*, Phys. Rev. B **57**, 9015 (1998).
[10] Y. Hasegawa and Ph. Avouris, Phys. Rev. Lett. **71**, 1071 (1993).
[11] M. F. Crommie *et al.*, Nature (London) **363**, 524 (1993).
[12] N. Sato *et al.*, Phys. Rev. B **59**, 2035 (1999).
[13] R. I. G. Uhrberg *et al.*, Phys. Rev. B **65**, 081305(R) (2002).
[14] M. Ono *et al.*, Phys. Rev. B **67**, 201306(R) (2003).
[15] Peaks around -0.5 V found in the inset of Fig. 2(a) are temporarily attributed to the $S2$ state at the $\bar{M}$ point. The position of the peaks behaves in a similar manner with those around -0.85 V.
[16] T. Nagao *et al.*, Phys. Rev. Lett. **86**, 5747 (2001).
[17] N. Sato *et al.*, Phys. Rev. B **60**, 16 083 (1999).
[18] The potential profile is actually not sensitive to the atomic positions of the adsorbed Ag atoms in the cluster, since the characteristic length of the potential variation, namely, the half wavelength, is rather large compared with the separation among the Ag atoms. Therefore, the agreements between the theory and experiments do not claim that the structural model we assumed is correct.
[19] In estimating the charge amounts, we assumed that the charges were located in the same plane as the 2DEG. If the charges were located at distance d from the plane, the potential should be multiplied by $1 + 2d/a_B$. When the charges are located on a terrace higher by one atomic step ($d = 0.31$ nm), $1 + 2d/a_B$ is $\sim$1.2, meaning that the charge amount is overestimated by $\sim$20%.
[20] S. J. Stranick *et al.*, Science **266**, 99 (1994).
[21] M. M. Kamna *et al.*, Science **274**, 118 (1996).
[22] J. Repp *et al.*, Phys. Rev. Lett. **85**, 2981 (2000).
[23] F. Silly *et al.*, Phys. Rev. Lett. **92**, 016101 (2004).